IJST, Transactions of Civil Engineering, Vol. 38, No. C1, pp 1-20
Printed in The Islamic Republic of Iran, 2014

OPTIMIZATION OF SKELETAL STRUCTURES USING A HYBRIDIZED ANT COLONY-HARMONY SEARCH- GENETIC ALGORITHM*

M. H. TALEBPOUR[1], A. KAVEH[2**] AND V. R. KALATJARI[3]

[1, 3]Dept. of Civil Engineering, Shahrood University of Technology, Shahrood, I. R. of Iran
[2]Centre of Excellence for Fundamental Studies in Civil Engineering, Iran University of Science and Technology, Tehran, I. R. of Iran
Email: alikaveh@iust.ac.ir

Abstract– Ant Colony Optimization (ACO) has been used as one of the popular meta-heuristic algorithms in structural optimization. In this algorithm, the selected cross sections are chosen according to a parameter called "probability ratio". This parameter and the way to choose the cross sections from a list of cross sections, are the most important points in the optimization process. Though the Ant Colony algorithm has a special ability in achieving the optimal point, in some cases in order to avoid local optima, the utilization of special techniques is needed. In the present paper, the first aim is to use Harmony Search (HS) algorithm to increase the local search ability of the ACO. In this way a combined algorithm, denoted by HACOHS, is obtained with special abilities to achieve a global optimum. For this purpose, optimal design of skeletal structures such as trusses and steel frames is considered using the HACOHS. However, in the process of optimization by HACOHS method, several GA selections are employed at the cross section selection stage**.** Utilizing the Tournament (HACOHS-T), Roulette wheel (HACOHS-Ro), and Rank (HACOHS-Ra) methods it is found that the HACOHS-T is the most efficient of these algorithms for optimal design of skeletal structures.

Keywords– Optimization, ant colony algorithm, harmony search, genetic algorithm, skeletal structures

1. INTRODUCTION

In the last two decades, meta-heuristic algorithms have been used extensively in optimal design of structures. These algorithms are intelligent random search approaches, mostly based on some processes and rules from nature. The logic of these algorithms is such that they investigate and search the entire design space point by point and progress to the optimum point through generating improved designs in optimization process without any restrictions on design variable type and problem constraints [1, 2]. The main idea of meta-heuristic methods was first exposed by Fogel through presenting an Evolution Strategy in 1966 [3]. Thereafter, other researchers presented several other algorithms each having their advantages and disadvantages. These algorithms which were inspired by natural processes consisted of GA, ACO, HS [4-8]. In recent years, the performance of these algorithms has improved and their shortcomings are reduced by combining different meta-heuristic approaches [9-12].

Ant colony algorithm is known as an efficient meta-heuristic method with good performance [13, 14]. This method was first introduced by Colorni et al. [6, 7] as Ant System (AS) to solve the travelling salesman problem. The main logic of the method was based on the inspiration of ants' behavior searching for food. Ants as social blind insects live in a society with mutual cooperation and use a chemical substance called pheromone to discover the shortest route towards the food source. Each insect leaves a

*Received by the editors September 25, 2012; Accepted March 18, 2013.
**Corresponding author

small amount of pheromone from place to place to identify the way back and also facilitate the route determination for the other ants and return to formicary from the previous route.

The more the pheromone of a route, the greater the chance for other ants to choose the same route. Consequently, the path to reach the food source may have a greater chance to reinvest the pheromone and also be chosen by other ants. Pheromone rate of each path constantly changes proportional to the passing rate of the other ants and also by the magnitude of the evaporation. Evaporation process results in eliminating the long and unsuccessful routes during ants search action so that the shortest path to the food source will be detected by ants. Inspired by this fact, structural optimization problem was investigated by several researchers and in some cases the standard algorithm is improved through some enhancements [15-18]. In this relation, different approaches based on Ant Colony algorithm principles namely, Ant Colony System (ACS), Max-Min Ant System (MMAS), Rank-Based Ant System (RBAS), Best and Worst Ant System (BWAS) were proposed by different researchers [19-21]. In most cases, the ability of the Ant Colony algorithm in obtaining the optimal point (global search) has been improved and even in some cases its local search ability is also enhanced.

Harmony Search algorithm is best known for its local search ability within the range of optimum design. Lee and Jim (2001) proposed this method, which is inspired by the process that a musician follows to search for an appropriate status while playing music [8].

According to this algorithm, each musician is replaced by design variable during optimization process and entire musicians form the design variables vector. Beauty and quality of the music results in the objective function value for the vector of design variables. In structural optimization process based on the HS, a primary population without constraint violations is required to detect optimum points in the vicinity of the present population and to replace them instead of its members based on parameters such as *HMCR*, *PAR* and *bw* [22, 23]. Therefore, several iterations are required for this method to generate a primary population and also to achieve the global optimum point, and it is considered as an appropriate method for local search within the optimum point range. Thus combining HS and ACO methods may result in a high performance algorithm with global and local search capabilities to achieve a global optimum point.

On the other hand, in a structural optimization based on the ACO, cross sections from the list of sections are selected according to a parameter called probability ratio which is similar to the roulette wheel selection method of the Genetic algorithm. Accordingly, sections with higher pheromone rate have a greater chance to be selected. Investigations on GA reveal that in some cases other selection methods such as tournament method produce better results and lead to a more suitable optimum point [24].

The present research is concerned with optimal design of frame and truss structures based on a combined algorithm of Ant Colony and Harmony Search. The performance of the HACOHS is improved through using different approaches for the selection process in GA for selecting appropriate cross sections from the section. For this purpose, the roulette wheel (HACOHS-RO), tournament (HACOHS-T) and rank (HACOHS-RA) methods are utilized and the convergence path to attain an optimum point is used as a criterion for comparison of the above mentioned methods. Results indicate that the use of HACOHS-T method improves the resulting responses of the optimum structures.

2. STRUCTURAL OPTIMIZATION BASED ON HACOHS

Optimization process based on the HACOHS method is almost similar to the ACO algorithm; however, the local search process is performed with exerting a condition as local search condition of the HS method. Figure 1 illustrates the flowchart of the HACOHS algorithm.

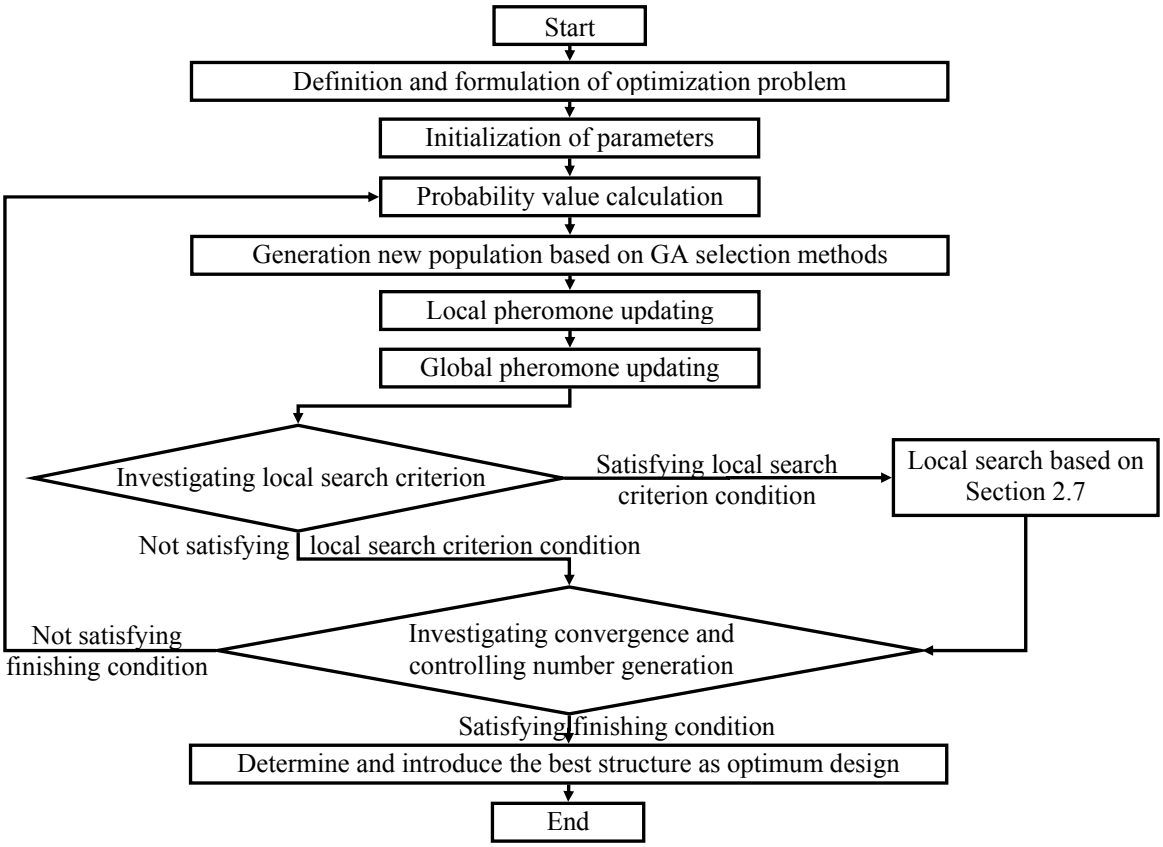

Fig. 1. Structural optimization algorithm by HACOHS

a) Formulation of the optimization problem

Optimal design of skeletal structures is formulated as follows:
Find the least value of the weight objective function under the constraints C1 and C2:

$$W(A) = \sum_{i=1}^{Ne} (\rho_i l_i a_i) \tag{1}$$

$$\text{C1} : |\sigma_j| \le |\sigma_j^{all}| \qquad j = 1, 2, \ldots, Ne \tag{2}$$

$$\text{C2} : |\Delta_k| \le |\Delta_k^{all}| \qquad k = 1, 2, \ldots, Ndof \tag{3}$$

In Eq. (1), a vector of cross section variables, the matrix [*A*], is defined as:

$$[A]=[a_1, a_2, \ldots, a_{Nos}] \quad ; \quad a_i \in S \quad ; \quad i=1, \ldots, Nos \tag{4}$$

In Eq. (1) to Eq. (4), ρ_i is the materials density of the *i*th member, l_i is the length of the i^{th} member, a_i is cross section for the i^{th} member and *Ne* is number of structural members. *S* is the list of available profiles found for the numbers of *Ns* from which the optimum designs are chosen. *Nos* is the number of sections for each design which is determined according to the structural members grouping. σ_j shows stress value of j^{th} member and σ^{all} is the value of allowable stress. Δ_k indicates displacement of k^{th} degree of freedom and Δ^{all}_k is maximum displacement of k^{th} degree of freedom. *NDOF* is the number of active degrees of freedom for active joints of the structure.

Constraint C1: In an optimum structure, stress raised from load combinations in all members must be in the allowable range which is determined based on the code being used. Accordingly, stress value of each member of the structure in the optimization process is controlled. Violation of the stress constraint is

determined by Eq. (5). In *nlc* number of load combinations status, values of the constraint violation of all the members are added together.

$$C3=\begin{cases} C_3^{\,i}=0 \quad if \quad \left|\dfrac{\sigma_i}{\sigma_{all}}\right|-1\le 0 \quad ; \quad i=1,..,Ne \\ C_3^{\,i}=\left|\dfrac{\sigma_i}{\sigma_{all}}\right|-1 \quad if \quad \left|\dfrac{\sigma_i}{\sigma_{all}}\right|-1>0 \quad ; \quad i=1,..,Ne \end{cases} \tag{5}$$

Constraint C2: After structural analysis and calculating the stresses, the displacements of the active nodes in each design are calculated. If the i^{th} degree of freedom displacement is in the range, no penalty will be considered; otherwise, the design will be penalized proportional to the violation. The violation of the displacement constraint is determined by Eq. (6). In the load combinations status, the violations of the nodal displacement constraints are also added together for *nlc* cases.

$$C4=\begin{cases} C_4^{i}=0 \quad if \quad \left|\dfrac{\Delta_i}{\Delta_i^{all}}\right|-1\le 0 \quad ; \quad i=1,..,Ndof \\ C_4^{i}=\left|\dfrac{\Delta_i}{\Delta_i^{all}}\right|-1 \quad if \quad \left|\dfrac{\Delta_i}{\Delta_i^{all}}\right|-1>0 \quad ; \quad i=1,..,Ndof \end{cases} \tag{6}$$

b) Initialization of the parameters

The present combined algorithm (HACOHS) at first needs parameter initialization similar to the other meta-heuristic algorithms. In this algorithm, in addition to the initial parameters of the Ant Colony algorithm such as the number of members, α, β, evaporation rate, and the parameters of the Harmony Search consisting of *PAR*, *HMCR* are also initialized. Moreover, the local search criterion which provides search terms through HS method is also determined.

At this stage, the amount of primary pheromone for all possible status will be initialized. Since there is a choice for the number of sections listed for each member of structures, a matrix called T with dimensions proportional to the number of sections from the available list and the number of design variables (number of structural member grouping) will be developed as Eq. (7) to determine the pheromone value. Each element of this matrix (T_{ij}) indicates the amount of pheromone rate of the i^{th} state from the list of sections for the j^{th} design variable.

$$T=\begin{bmatrix} T_{11} & T_{12} & \cdots & T_{1Nos} \\ T_{21} & T_{22} & \cdots & T_{2Nos} \\ \vdots & \vdots & & \\ T_{Ns1} & T_{Ns2} & \cdots & T_{NsNos} \end{bmatrix}_{Ns\times Nos} \tag{7}$$

The amount of the primary pheromone in this matrix is initialized according to Eq. (8).

$$T_{ij}^{0}=\frac{1}{W_{\min}} \tag{8}$$

Where W_{min} is the value of the objective function accounted for the first state of the list of sections to all the design variables [25].

c) Probability value calculation

Following the initialization of the parameters of the combined algorithm, selection probability of each current mode (proportional to sections list) for each design variable is calculated as follows [17]:

$$p_{ij} = \frac{[T_{ij}]^{\alpha}[\upsilon_i]^{\beta}}{\sum_{k=1}^{Ns}[T_{kj}]^{\alpha}[\upsilon_k]^{\beta}} \quad i = 1,\ldots,Ns \quad ; \quad j = 1,\ldots,Nos \tag{9}$$

Where P_{ij} is the selection probability of the i^{th} mode (path) for the j^{th} design variable. v_i is the stability coefficient for the i^{th} mode from the list of sections which is defined as [25]:

$$\upsilon_i = \frac{1}{a_i} \quad ; \quad a_i \in S \quad ; \quad i = 1,\ldots,Ns \tag{10}$$

As can be seen from Eq. (10) the lower the a_i value, the more v_i is and correspondingly p_{ij} increase with the increase of v_i according to Eq. 9.

In Eq. (9), α and β are two parameters that weigh the relative importance of the pheromone trail and the heuristic information, respectively. If $\alpha = 0$, then p_{ij} will be proportional to v_i value and correspondingly proportional to the selected cross section value (a_i). Therefore, the optimization process becomes randomized. On the other hand, if $\beta = 0$, then only the pheromone impact will be effective in the choice probability function which can result in a rapid and early convergence and as a consequence, increases the probability of obtaining a local optimum [25].

d) Generating new population based on the GA selection methods

In the HACOHS algorithm, after calculating the values of the selection probability, new population should be determined based on the p_{ij} values. Therefore, in the present paper, many different selection methods of GA [24] are investigated and utilized.

HACOHS-RO: Roulette Wheel procedure of GA is used in this method [26]. Accordingly, the sum of p_{ij} values for the i^{th} design variable is equal to 1. Now, if the probability obtained for the j^{th} design variable is depicted as a roulette wheel, p_{ij} values will form its sectors. Through generating an additional number between 0 and 1, a cross section from the sections list with larger sector may have a better chance to be selected. In order to implement this method, the cumulative probability of $\overline{P_i}$ for the j^{th} design variable is determined as follows:

$$\overline{P}_i^{\,j} = \sum_{k=1}^{i} P_{kj} \quad ; \quad i = 1,\ldots Ns \tag{11}$$

Now a random number is produced between 0 and 1. The selected cross section is identified from the list of sections by comparing the random number to $\overline{P_i}^{\,j}$ values. This procedure is performed for all the design variables to form the new design. The process is repeated for all the population to form the new population based on the p_{ij} value according to T_{ij}.

HACOHS-Ra: Ranking technique of GA is used to select cross section from the list of sections [27]. The p_{ij} values are ordered from smallest to largest values. For instance, the worst cross section with the lowest probability ratio possesses the first rank and likewise continues. Finally, the best cross section with the highest probability ratio will have ranking equal to *Ns*. Then cross section selection is performed based on member ranking in the arranged list and secondary probability ratio is estimated as follows:

$$P'_{ij} = \frac{m}{\sum_{j=1}^{Ns} j} \tag{12}$$

Where *m* indicates the cross section member in the arranged list of sections according to p_{ij} value. In other words, *m* is equal to *i*. The cumulative values of $\overline{P_i}^{\,j}$, similar to the roulette wheel method, are determined

according to Eq. (11) and selected cross section for the j^{th} design variable is chosen by producing uniform numbers ranging from 0 to 1 and comparing to $\overline{P_i}^j$. This procedure is performed for all the design variables to take shape for the new design. The process is repeated for the number of population members to construct the new population.

HACOHS-T: In this method, tournament selection approach is used in GA to select cross section for the i^{th} design variable [28]. Accordingly, some cross sections, proportional to tournament size, are selected randomly for the i^{th} design variable and during a competition, a cross section from a list of sections is selected with the highest value of p_{ij} for the i^{th} design variable. This procedure is performed for all the design variables to form the new design. The process is repeated for the number of population members in order to form the new population based on p_{ij} value according to T_{ij} .

e) Local updating and fitness calculation

As illustrated in Eq. (13), following new population formation, pheromone rate corresponding to total selected cross sections (passed routes) for each design variable is decreased with a constant coefficient which prevents pheromone accumulation on each path and unfavorable and failed decisions are also ignored [25].

$$T_{ij}^{new} = \rho_0 T_{ij}^{old} \tag{13}$$

Where T_{ij}^{new} and T_{ij}^{old} are the *new* and *old* pheromone rates for passed routes, respectively. ρ_o is the local update coefficient which has a value ranging from 0 to 1.

The value of the objective function is estimated using Eq. (1), following the local upgrading. Applying the modified objective function, constraint optimization problem is converted to an unconstraint optimization problem which is described by the following equation:

$$\varphi(A) = W(A) \left[1 + K\left(\sum_{q=1}^{nlc}\sum^{Q} \max\left[0, Gq\right]\right)\right] \tag{14}$$

Where
$W(A)$: The objective function
Gq: The structural violation rate related to each constraint
$[A]$: The vector of design variables
Q: The total constraints governing the problem
nlc: The number of load combinations
K: The penalty constant

As can be deduced from Eq. (14), for every design that violates the problem constraints more, the corresponding φ function value will be more as well and will have lower fitness [29]. As a result, following the estimation of φ values corresponding to each design, the present population will be ranked merit-based [16].

f) Global updating and depositing pheromones

After ordering the present population based on fitness, the pheromone rate of all modes in the list of sections for all the design variables at global upgrading stage are decreased with a coefficient called evaporation rate. In the other words, all the pheromone matrix entries are reduced based on the following equation [15].

$$[T]^{new} = (1 - e_r)[T]^{old} \tag{15}$$

Where e_r indicates the pheromone global evaporation rate. *old* and *new* transcribers indicate old and new pheromone matrices, respectively.

After performing the global pheromone evaporation process, pheromone should be placed on the passed routes. In the present work, a small population, λ_r , of the best present population (μ) is primarily formed. λ_r value is initialized at the first stage. Afterwards, pheromone rate of the list of sections modes for design variables which are selected in the selection stage (passed routes) is increased as follows [25]:

$$T_{ij} = T_{ij} + e_r.\left[\lambda_r.(\Delta T_{ij})_{best} + \sum_{k=1}^{\lambda_r}(\lambda_r - r_k).(\Delta T_{ij})_k\right] \tag{16}$$

Where *ij* indicates the passed routes and r_k shows each design number in μ population so that r_k is always in the range of 1 to λ_r. $(\Delta T_{ij})^k$ represents the amount of pheromone needed to be placed in the *ij* route which depends on resulted response quality raised from k^{th} design and (ΔT_{ij}) best corresponds to the best design. (ΔT_{ij}) for k^{th} design is calculated as follows:

$$(\Delta \tau_{ij})_k = \frac{1}{\varphi(A)^k} \tag{17}$$

Where $\varphi(A)$ for the k^{th} design based on Eq. (14) is among the best. Considering Eq. (16), more pheromone is placed on the passed routes from μ population which results in an increase of the convergence rate in the present algorithm [25].

g) Local search

In the present paper, if no change is observed in successive generations of the optimization process in fitness value of the best population design and small μ population possesses designs with no constraint violation, then local search process inspired by HS method on the μ population is performed. To attain this, μ population designs called *HM* are placed in a matrix as follows:

$$HM = \begin{bmatrix} a_1^1 & a_2^1 & \dots & a_{Nos}^1 \\ a_1^2 & a_2^2 & \dots & a_{Nos}^2 \\ \vdots & \vdots & & \\ a_1^{\lambda_r} & x_2^{\lambda_r} & \dots & x_{Nos}^{\lambda_r} \end{bmatrix}_{\lambda_r \times Nos} \tag{18}$$

Then, for the number of *HM* population, new design variable vector $[A] = [a_1', a_2', \ldots, a_{Nos}']$ is formed, based on Fig. 2 according to the HS rules, *HCMR* and *PAR* parameters. If the new vector is better than the worst *HM* vector, it is replaced by the most incompetent *HM* design; otherwise *HM* stays unchanged.

Accordingly, every value of a'_i in the new vector $[A']$ can be based on the HMCR parameter or regenerated randomly, and/or can be determined based on a'_i - $a_i^{\lambda r}$ as corresponding values in *HM*.

This stage is performable through generating a random number between 0 and 1 (*Ran*1) and comparing to the *HMCR* value. If the random number is greater than 1, a'_i will be determined randomly from the list of sections; otherwise a'_i value is determined from *HM*. Determination of the a'_i from *HM* limit is also performed based on the *PAR* parameter. For this purpose, a'_i is determined by generating a random number between 0 and 1 (*Ran*2) and comparing with *PAR* value. If the random number is smaller than *PAR*, a'_i will be selected from the corresponding values in *HM*; otherwise value of the a'_i is determined from a corresponding value in the vicinity of a'_i in list of sections based on *bw* value [23, 30]. Full description of this method is illustrated in Fig. 2, where *FNs* shows a function which determines every cross section's number from the list of sections, and FNs^{-1} determines its inverse function.

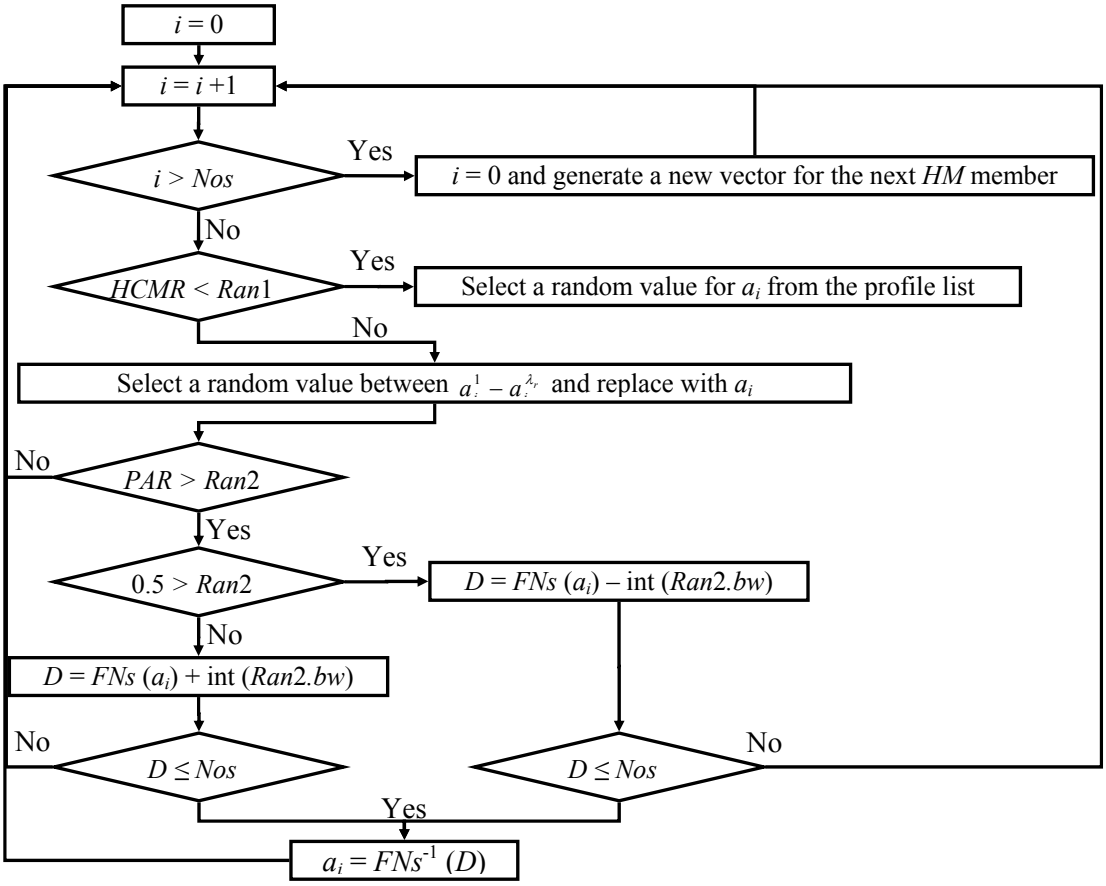

Fig. 2. Local search in the HACOHS

Hereafter, the entries of the pheromone matrix correspond to a range of possible scenarios in the list of sections for the *HM* members which are considered to be equal to the initial pheromone rate, and the remaining entries of the pheromone matrix are equated to zero. In other words, the pheromone corresponding to several cross sections on the top and bottom of the *HM* designs from list of sections in pheromone matrix is considered equal to the primary pheromone rate, and the remaining entries of the pheromone matrix are considered as zero [16]. The desired range for the neighborhood of the *HM* members is determined proportional to the value of the parameter *bw*.

h) Termination criterion

Several methods are available for termination condition in meta-heuristic algorithms [1]. In this paper, HACOHS termination condition is satisfied with controlling the number of iterations. After termination of the algorithm, the best design is obtained as the optimum design, and the convergence curve is drawn and thus an accurate comparison among different selected methods with HACOHS for each example is achieved.

3. NUMERICAL EXAMPLES

In this section, several examples of skeletal structures are optimized for evaluating the efficiency of the HACOHS-RO, HACOHS-RA and HACOHS-T. Here, three steel trusses and two steel frames are designed. To provide an accurate judgment and to avoid the effect of random parameters, the convergence diagrams for each example are drawn using an average of 30 different runs.

a) A 52-bar truss

Optimal design of a 52-bar truss, shown in Fig. 3, is performed as the first example. Here, E and ρ are assumed to be as 2.07×10^5 *MPa* and 7860 kg/m^3, respectively.

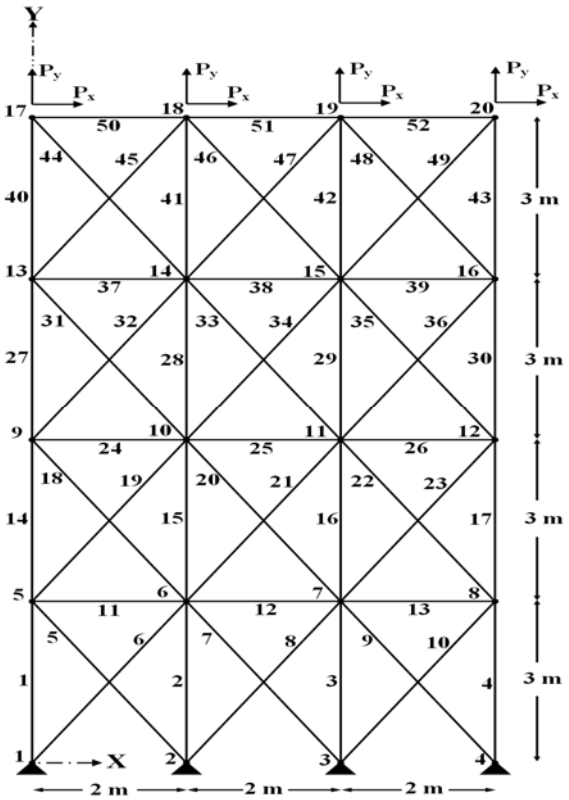

Fig. 3. A 52-bar planar truss structure.

In Fig. 3, the loads P_x and P_y are 100 *kN* and 200 *kN*, respectively. Here, the truss members are categorized into 12 groups and the allowable stress constraints are considered in the range of ±180 *MPa*. The sections of the 52-bar truss are listed in Table 1.

Table 1. The available cross-section areas of the AISC code

No.	in^2	mm^2	No.	in^2	mm^2	No.	in^2	mm^2	No.	in^2	mm^2
1	0.111	71.613	17	1.563	1008.385	33	3.840	2477.414	49	11.500	7419.430
2	0.141	90.968	18	1.620	1045.159	34	3.870	2496.769	50	13.500	8709.660
3	0.196	126.451	19	1.800	1161.288	35	3.880	2503.221	51	13.900	8967.724
4	0.250	161.290	20	1.990	1283.868	36	4.180	2696.769	52	14.200	9161.272
5	0.307	198.064	21	2.130	1374.191	37	4.220	2722.575	53	15.500	9999.980
6	0.391	252.258	22	2.380	1535.481	38	4.490	2896.768	54	16.000	10322.560
7	0.442	285.161	23	2.620	1690.319	39	4.590	2961.284	55	16.900	10903.204
8	0.563	363.225	24	2.630	1696.771	40	4.800	3096.768	56	18.800	12129.008
9	0.602	388.386	25	2.880	1858.061	41	4.970	3206.445	57	19.900	12838.684
10	0.766	494.193	26	2.930	1890.319	42	5.120	3303.219	58	22.000	14193.520
11	0.785	506.451	27	3.090	1993.544	43	5.740	3703.218	59	22.900	14774.164
12	0.994	641.289	28	1.130	729.031	44	7.220	4658.055	60	24.500	15806.420
13	1.000	645.160	29	3.380	2180.641	45	7.970	5141.925	61	26.500	17096.740
14	1.228	792.256	30	3.470	2238.705	46	8.530	5503.215	62	28.000	18064.480
15	1.266	816.773	31	3.550	2290.318	47	9.300	5999.988	63	30.000	19354.800
16	1.457	939.998	32	3.630	2341.931	48	10.850	6999.986	64	33.500	21612.860

Figure 4 shows the convergence curves of the present truss as an average of 30 different runs based on HACOHS-RO, HACOHS-RA and HACOHS-T methods. This confirms that the convergence rate of the HACOHS-T is higher. This method leads to lighter weight than the other existing approaches. Table 2 includes the results of the optimum design for the present algorithm and some other existing approaches.

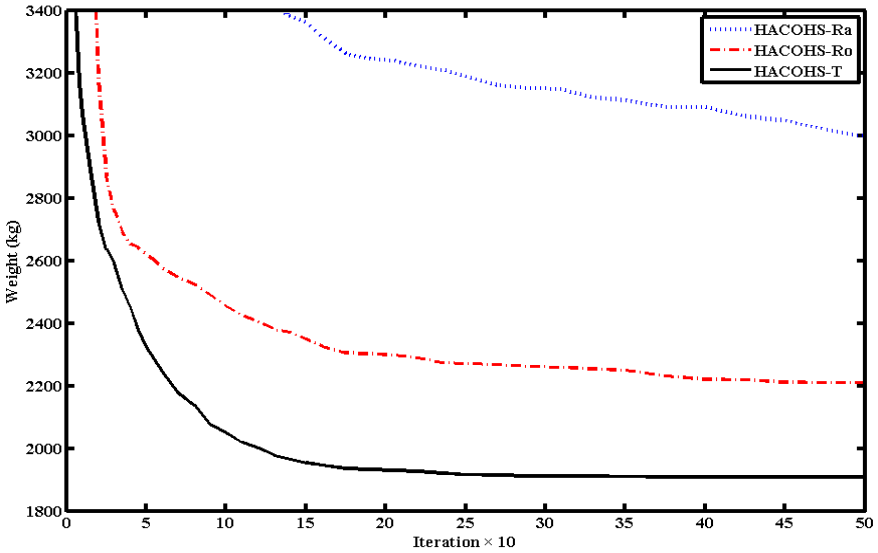

Fig. 4. The convergence history of the proposed methods for the 52-bar truss structure

Table 2. Comparison of the optimal designs for the 52-bar planar truss structure (mm^2)

Gr.	Mem.	Wu and Chow [31]	Lee and Geem [30]	Li et al. [32]	Li et al. [32]	Li et al. [32]	Kaveh and Talatahari [11]	Capriles et al. [16]	Kaveh and Talatahari [33]	This Study
		GA	HS	PSO	PSOPC	HPSO	DHPSACO	$RBAS_{LU,2}$	CSS	HACOHS-T
1	A_1-A_4	4658.055	4658.055	4658.055	5999.988	4658.055	4658.055	4658.055	4658.055	4658.055
2	A_5-A_{10}	1161.288	1161.288	1374.190	1008.380	1161.288	1161.288	1161.288	1161.288	1161.288
3	A_{11}-A_{13}	645.160	494.193	1858.060	2696.770	363.225	494.193	506.451	388.386	494.193
4	A_{14}-A_{17}	3303.219	3303.219	3206.440	3206.440	3303.219	3303.219	3303.219	3303.219	3303.219
5	A_{18}-A_{23}	1045.159	939.998	1283.870	1161.290	940.000	1008.385	940.000	940.000	939.998
6	A_{24}-A_{26}	494.193	641.289	252.260	729.030	494.193	285.161	506.451	494.193	494.193
7	A_{27}-A_{30}	2477.414	2238.705	3303.220	2238.710	2238.705	2290.318	2238.705	2238.705	2238.705
8	A_{31}-A_{36}	1045.159	1008.385	1045.160	1008.380	1008.385	1008.385	1008.385	1008.385	1008.385
9	A_{37}-A_{39}	285.161	363.225	126.450	494.190	388.386	388.386	388.386	494.193	494.193
10	A_{40}-A_{43}	1696.771	1283.868	2341.93	1283.870	1283.868	1283.868	1283.868	1283.868	1283.868
11	A_{44}-A_{49}	1045.159	1161.288	1008.38	1161.290	1161.288	1161.288	1161.288	1161.288	1161.288
12	A_{50}-A_{52}	641.289	494.193	1045.16	494.190	792.256	506.451	506.451	494.193	494.193
	Gq	--	--	--	--	--	0.002725	0.000116	0.001143	--
	Weight-*kg*	**1970.142**	**1903.36**	**2230.16**	**2146.63**	**1905.495**	**1904.83**	**1899.35**	**1897.62**	**1902.605**

b) A 72-bar truss

In this example, the optimal design of a 72-bar truss, shown in Fig. 5, is performed. Here, E and ρ are considered as 10000 *ksi* (68947.6 *MPa*) and 0.1 lb/in^3 (2767.99 kg/m^3), respectively. The stress range for truss members, and the maximum nodal displacement are limited to ±25 *ksi* (±172.369 *MPa*) and ±0.25 *in* (0.635 *Cm*), respectively. Present truss members are categorized into 16 groups. Table 1 contains the list of sections, and Table 3 shows the applied loads for 2 different conditions.

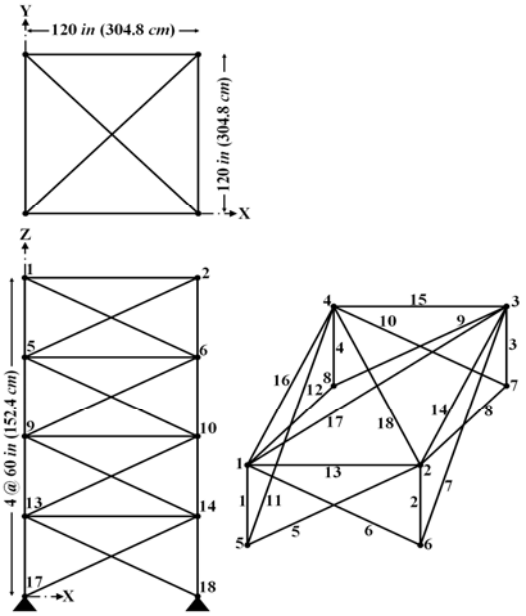

Fig. 5. A 72-bar spatial truss structure

Table 3. Loading conditions for the 72-bar spatial truss structure

Nodes	Condition 1			Condition 2		
	P_x *kips* (*kN*)	P_y *kips* (*kN*)	P_z *kips* (*kN*)	P_x *kips* (*kN*)	P_y *kips* (*kN*)	P_z *kips* (*kN*)
17	5.0 (22.241)	5.0 (22.241)	–5.0 (–22.241)	0	0	–5.0 (–22.241)
18	0	0	0	0	0	–5.0 (–22.241)
19	0	0	0	0	0	–5.0 (–22.241)
20	0	0	0	0	0	–5.0 (–22.241)

Figure 6 illustrates the convergence curve for an average of 30 runs of the proposed methods. From this figure it can be deduced that HACOHS-T method is more successful and also possesses a higher chance of obtaining lighter designs than the other proposed methods.

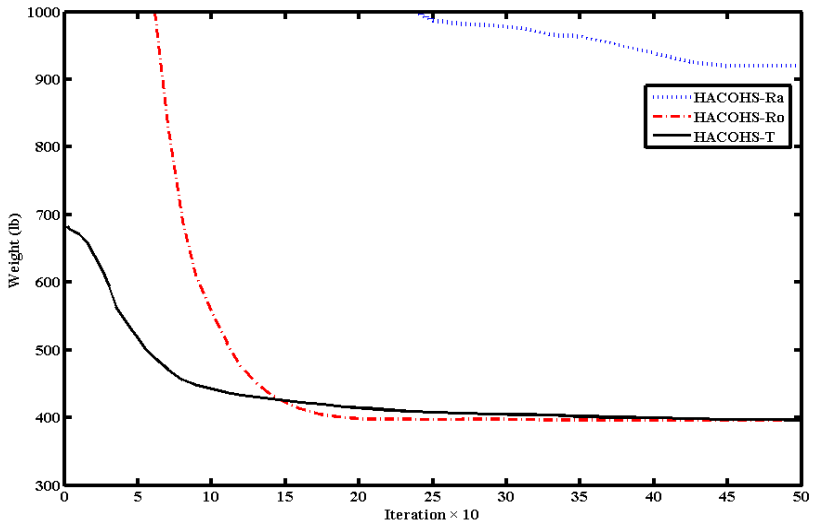

Fig. 6. The convergence history of the proposed methods for the 72-bar truss structure

The best design for the 72-bar truss is also obtained by HACOHS-T. Table 4 includes the results of the optimum design for the HACOHS-T in comparison to those of the other methods. It is obvious that the proposed method leads to lower weight design than the other algorithms.

Table 4. Comparison of the optimal designs for the 72-bar spatial truss structure

Gr.	Mem.	Optimal cross-sectional area – in^2 (mm^2)							
		Wu and Chow [31]	Li et al. [32]	Li et al. [32]	Li et al. [32]	Kaveh and Talatahari [11]	Kaveh and Talatahari [33]	Kalatjari and Talebpour [29]	This Study
		GA	PSO	PSOPC	HPSO	DHPSACO	CSS	M.S.M	HACOHS-T
1	A_1-A_4	0.196 (126.451)	7.220 (4658.055)	4.490 (2896.768)	4.970 (3206.445)	1.800 (1161.288)	1.990 (1283.868)	1.990 (1283.868)	1.563 (1008.385)
2	A_5-A_{12}	0.602 (388.386)	1.800 (1161.288)	1.457 (939.998)	1.228 (792.256)	0.442 (285.161)	0.442 (285.161)	0.602 (388.386)	0.563 (363.225)
3	A_{13}-A_{16}	0.307 (198.064)	1.130 (729.031)	0.111 (71.613)	0.111 (71.613)	0.141 (90.968)	0.111 (71.613)	0.111 (71.613)	0.111 (71.613)
4	A_{17}-A_{18}	0.766 (494.193)	0.196 (126.451)	0.111 (71.613)	0.111 (71.613)	0.111 (71.613)	0.111 (71.613)	0.111 (71.613)	0.111 (71.613)
5	A_{19}-A_{22}	0.391 (252.258)	3.090 (1993.544)	2.620 (1690.319)	2.880 (1858.061)	1.228 (792.256)	0.994 (641.289)	1.266 (816.773)	1.266 (816.773)
6	A_{23}-A_{30}	0.391 (252.258)	0.785 (506.451)	1.130 (729.031)	1.457 (939.998)	0.563 (363.225)	0.563 (363.225)	0.442 (285.161)	0.563 (363.225)
7	A_{31}-A_{34}	0.141 (90.968)	0.563 (363.225)	0.196 (126.451)	0.141 (90.968)	0.111 (71.613)	0.111 (71.613)	0.111 (71.613)	0.111 (71.613)
8	A_{35}-A_{36}	0.111 (71.613)	0.785 (506.451)	0.111 (71.613)	0.111 (71.613)	0.111 (71.613)	0.111 (71.613)	0.111 (71.613)	0.111 (71.613)
9	A_{37}-A_{40}	1.800 (1161.288)	3.090 (1993.544)	1.266 (816.773)	1.563 (1008.385)	0.563 (363.225)	0.563 (363.225)	0.442 (285.161)	0.391 (252.258)
10	A_{41}-A_{48}	0.602 (388.386)	1.228 (792.256)	1.457 (939.998)	1.228 (792.256)	0.563 (363.225)	0.563 (363.225)	0.602 (388.386)	0.563 (363.225)
11	A_{49}-A_{52}	0.141 (90.968)	0.111 (71.613)	0.111 (71.613)	0.111 (71.613)	0.111 (71.613)	0.111 (71.613)	0.111 (71.613)	0.111 (71.613)
12	A_{53}-A_{54}	0.307 (198.064)	0.563 (363.225)	0.111 (71.613)	0.196 (126.451)	0.250 (161.290)	0.111 (71.613)	0.111 (71.613)	0.111 (71.613)
13	A_{55}-A_{58}	1.563 (1008.385)	1.990 (1283.868)	0.442 (285.161)	0.391 (252.258)	0.196 (126.451)	0.196 (126.451)	0.196 (126.451)	0.196 (126.451)
14	A_{59}-A_{66}	0.766 (494.193)	1.620 (1045.159)	1.457 (939.998)	1.457 (939.998)	0.563 (363.225)	0.563 (363.225)	0.563 (363.225)	0.563 (363.225)
15	A_{67}-A_{70}	0.141 (90.968)	1.563 (1008.385)	1.228 (792.256)	0.766 (494.193)	0.442 (285.161)	0.442 (285.161)	0.391 (252.258)	0.391 (252.258)
16	A_{71}-A_{72}	0.111 (71.613)	1.266 (816.773)	1.457 (939.998)	1.563 (1008.385)	0.563 (363.225)	0.766 (494.193)	0.442 (285.161)	0.602 (388.386)
Weight-*lb* (*kg*)		**427.203 (193.776)**	**1209.48 (548.611)**	**941.82 (427.202)**	**933.09 (423.243)**	**393.380 (178.434)**	**393.05 (178.284)**	**391.607 (177.63)**	**390.18 (176.983)**

c) A 200-bar truss

This example deals with optimization of a 200-bar truss, as illustrated in Fig. 7. Here, E and ρ are assumed to be 30000 *Ksi* (206842.8 *MPa*) and 0.283 lb/in^3 (7833.412 kg/cm^3), respectively.

The truss members are categorized into 29 groups, and the allowable stress is taken as ±10 *ksi* (±68.9476 *MPa*). The external loads are exerted to the truss in 3 different conditions: (1) 1 *kip* (4.448 *kN*) load exerts to nodes 1, 6, 15, 20, 29, 34, 43, 48, 57, 62, 71 in x direction. (2) −10 *kip* (44.48 *kN*) load exerts to nodes 1, 2, …, 6, 8, 10, 12, 14, 15, …, 20, 22, 24, 25, …, 73, 74 and 75 in y direction. (3) Combination of conditions 1 and 2. The available list for optimization of the 200-bar truss is as follows:

$a_i \in$ S= {0.1 (64.516), 0.347 (223.8705), 0.44 (283.8704), 0.539 (347.7412), 0.954 (615.4826), 1.081 (697.4179), 1.174 (757.4178), 1.333 (859.9982), 1.488 (959.998), 1.764 (1138.0622), 2.142 (1381.9327), 2.697 (1739.9965), 2.8 (1806.448), 3.131 (2019.9959), 3.565 (2299.9954), 3.813 (2459.995), 4.805 (3099.9937), 5.952 (3839.9923), 6.572 (4239.9915), 7.192 (4639.9907), 8.525 (5499.989), 9.3 (5999.988), 10.85 (6999.986), 13.33 (8599.9828), 14.29 (9219.3363), 17.17 (11077.3972), 19.18 (12374.1688), 23.68 (15277.3887), 28.08 (18116.0928), 33.7 (21741.892)} in^2 - (mm^2); i = 1, …, 29.

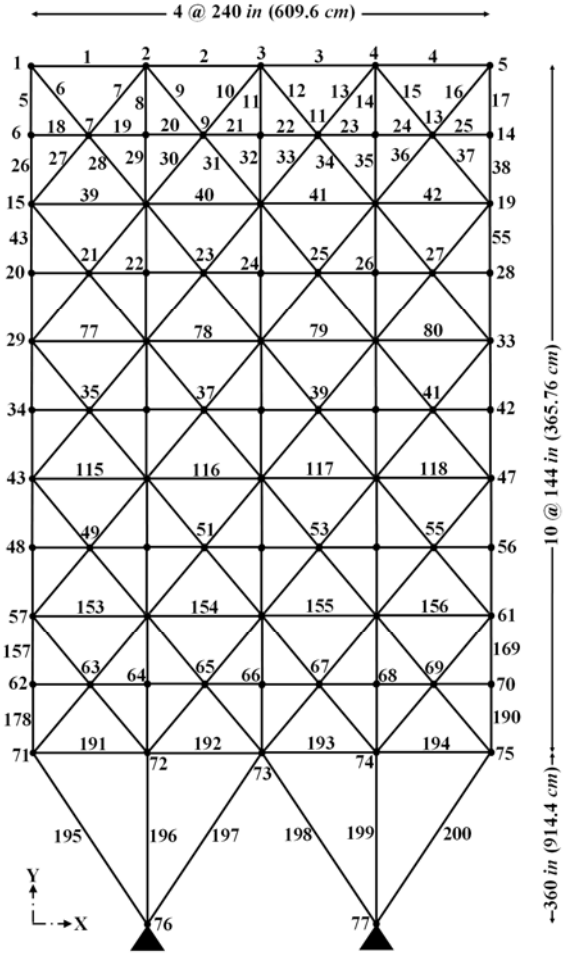

Fig. 7. A 200-bar planar truss structure

Figure 8 shows the convergence curves obtained by different proposed methods indicating a better convergence for the HACOHS-T. To avoid the effect of random parameters on the proposed methods, convergence curves for each method are drawn as the average of 30 runs. According to Table 5, the results of the HACOHS-T method confirm the better performance of this method.

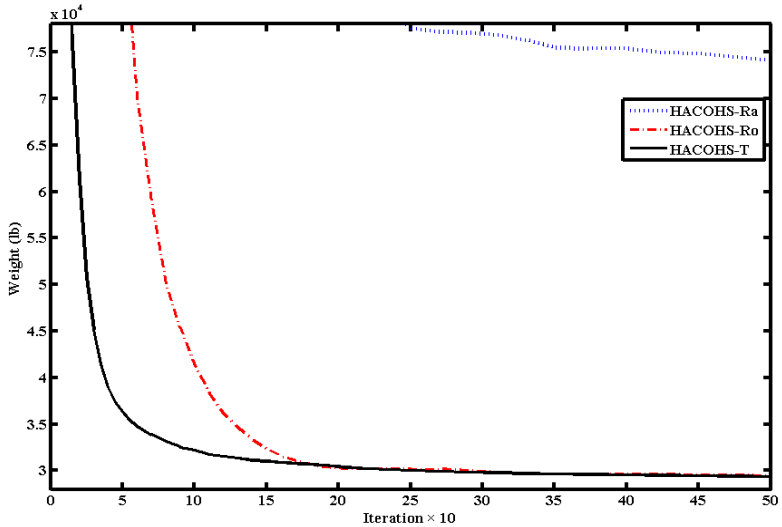

Fig. 8. The convergence history of the proposed methods for the 200-bar truss structure

Table 5. Comparison of the optimal designs for the 200-bar planar truss structure

Gr.	Members	Optimal cross-sectional area – in^2 (mm^2)			
		Coello and Christiansen [34]	Toğan and Daloğlu [35]	Kalatjari and Talebpour [36]	This study
		GA	GA	M.S.M	HACOHS-T
1	1, 2, 3, 4	--	0.347 (223.8705)	0.347 (223.8705)	0.1 (64.516)
2	5, 8, 11, 14, 17	--	1.081 (697.4179)	0.954 (615.4826)	1.081 (697.4179)
3	19, 20, 21, 22, 23, 24	--	0.1 (64.516)	0.1 (64.516)	0.347 (223.8705)
4	18, 25, 56, 63, 94, 101, 132, 139, 170, 177	--	0.1 (64.516)	0.1 (64.516)	0.1 (64.516)
5	26, 29, 32, 35, 38	--	2.142 (1381.9327)	2.142 (1381.9327)	2.142 (1381.9327)
6	6, 7, 9, 10, 12, 13, 15, 16, 27, 28, 30, 31, 33, 34, 36, 37	--	0.347 (223.8705)	0.347 (223.8705)	0.347 (223.8705)
7	39, 40, 41, 42	--	0.1 (64.516)	0.1 (64.516)	0.1 (64.516)
8	43, 46, 49, 52, 55	--	3.565 (2299.9954)	3.131 (2019.9959)	3.131 (2019.9959)
9	57, 58, 59, 60, 61, 62	--	0.347 (223.8705)	0.1 (64.516)	0.1 (64.516)
10	64, 67, 70, 73, 76	--	4.805 (3099.9937)	4.805 (3099.9937)	4.805 (3099.9937)
11	44, 45, 47, 48, 50, 51, 53, 54, 65, 66, 68, 69,71,72, 74, 75	--	0.44 (283.8704)	0.44 (283.8704)	0.44 (283.8704)
12	77, 78, 79, 80	--	0.44 (283.8704)	0.347 (223.8705)	0.1 (64.516)
13	81, 84, 87, 90, 93	--	5.952 (3839.9923)	5.952 (3839.9923)	5.952 (3839.9923)
14	95, 96, 97, 98, 99, 100	--	0.347 (223.8705)	0.1 (64.516)	0.1 (64.516)
15	102, 105, 108, 111, 114	--	6.572 (4239.9915)	6.572 (4239.9915)	6.572 (4239.9915)
16	82, 83, 85, 86, 88, 89, 91, 92, 103, 104, 106, 107, 109, 110, 112 ,113	--	0.954 (615.4826)	0.954 (615.4826)	0.539 (347.7412)
17	115, 116, 117, 118	--	0.347 (223.8705)	0.347 (223.8705)	1.174 (757.4178)
18	119, 122, 125, 128, 131	--	8.525 (5499.989)	8.525 (5499.989)	8.525 (5499.989)
19	133, 134, 135, 136, 137, 138	--	0.1 (64.516)	0.1 (64.516)	0.1 (64.516)
20	140, 143, 146, 149, 152	--	9.3 (5999.988)	9.3 (5999.988)	9.3 (5999.988)
21	120, 121, 123, 124, 126, 127, 129, 130, 141, 142, 144, 145, 147, 148, 150, 151	--	0.954 (615.4826)	0.954 (615.4826)	1.333 (859.9982)
22	153, 154, 155, 156	--	1.764 (1138.0622)	1.488 (959.998)	0.539 (347.7412)
23	157, 160, 163, 166, 169	--	13.33 (8599.9828)	13.33 (8599.9828)	13.33 (8599.9828)
24	171, 172, 173, 174, 175, 176	--	0.347 (223.8705)	0.347 (223.8705)	1.174 (757.4178)
25	178, 181, 184, 187, 190	--	13.33 (8599.9828)	13.33 (8599.9828)	13.33 (8599.9828)
26	158, 159, 161, 162, 164, 165, 167, 168, 179, 180, 182, 183, 185, 186, 188, 189	--	2.142 (1381.9327)	2.697 (1739.9965)	2.697 (1739.9965)
27	191, 192, 193, 194	--	4.805 (3099.9937)	3.813 (2459.995)	3.565 (2299.9954)
28	195, 197, 198, 200	--	9.3 (5999.988)	8.525 (5499.989)	8.525 (5499.989)
29	196 , 199	--	17.17 (11077.3972)	17.17 (11077.3972)	17.17 (11077.3972)
	Weight-*lb* (*kg*)	**36167.73 (160882.07)**	**28544.014 (12947.347)**	**28038.56 (12718.077)**	**28030.20 (12714.285)**

d) An eight-story, one-bay frame

In this example, an eight-story frame with one bay, as illustrated in Fig. 9, is optimized. Here, E and ρ are assumed as 200 GPa and 76.8 kN/m^3, respectively, and the lateral drift at the top of the structure is the only performance constraint (limited to 5.08 cm). Effective loads are considered for one condition as shown in Fig. 9. Members of the mentioned frame are categorized into 8 groups selected from a list of 268-sections (Table 6).

Table 6. The available cross-section areas of the AISC W-Section

No.	Section	A cm^2 (in^2)	I_x cm^4 (in^4)	S_x cm^3 (in^3)	I_y cm^4 (in^4)	S_y cm^3 (in^3)
1	W44 x 335	634.1923 (98.3)	1294479.734 (31100)	23105.76 (1410)	49947.771 (1200)	2458.059 (150)
2	W44 x 290	553.5473 (85.8)	1127987.163 (27100)	20319.959 (1240)	43704.299 (1050)	2179.479 (133)
⋮	⋮	⋮	⋮	⋮	⋮	⋮
267	W5 x 16	30.1934 (4.68)	886.573 (21.3)	139.454 (8.51)	312.589 (7.51)	20.811 (1.27)
268	W4 x 13	24.7096 (3.83)	470.341 (11.3)	89.473 (5.46)	160.665 (3.86)	16.387 (1)

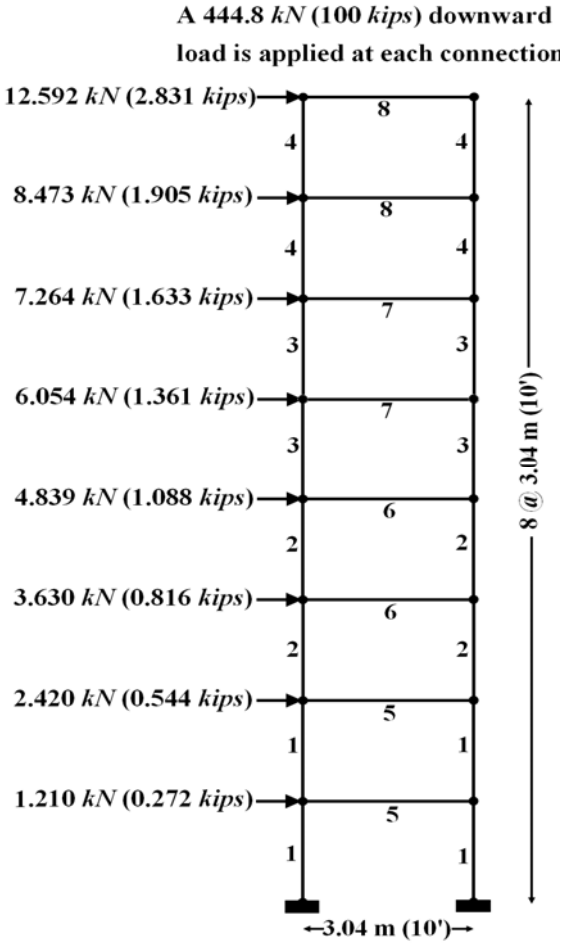

Fig. 9. A one-bay eight-story frame structure

Different proposed methods were applied to the optimal design of this frame, and the average of 30 different runs is used for drawing the convergence curves, Fig. 10. As it is shown in this figure, the HACOHS-T method has a better average performance than the other methods in obtaining the optimum design.

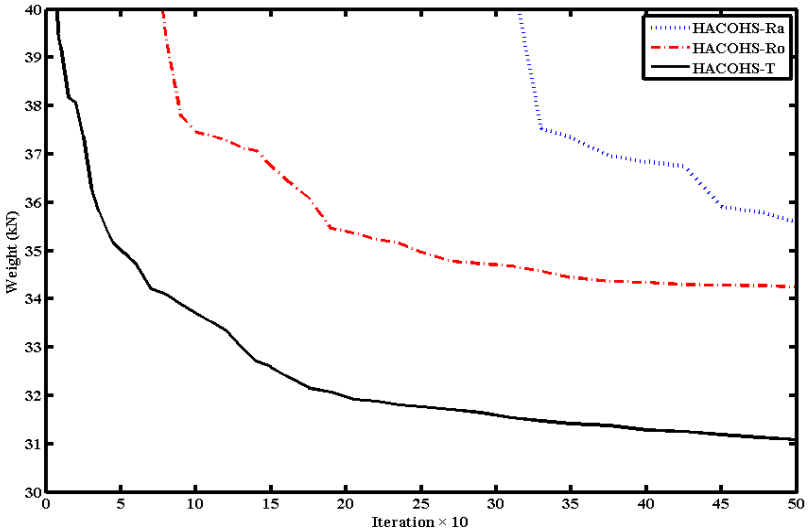

Fig. 10. The convergence history obtained by the proposed methods for the one-bay, eight story frame

The results indicate that the proposed HACOHS-T method is more efficient than the methods of the other researchers (Table 7).

Table 7. Comparison of optimal designs for the one-bay, eight story frame

Gr.	Khot et al [37]	Kaveh et al [12]	Camp et al [38]	Kaveh et al [9]	Kaveh et al [15]	Kaveh et al [12]	Kaveh et al [12]	Kaveh et al [17]	Kaveh et al [9]	This Study
	GA	PSO	FEAPGEN	PSOPC+ACO	ACO	GA	HGAPSO	ACO	DPSACO	HACOHS-T
1	W14 x 34	W21 x 44	W18 x 46	W18 x 35	W21 x 50	W21 x 44	W18 x 35	W18 x 40	W18 x 35	W 18 x 35
2	W10 x 39	W16 x 26	W16 x 31	W16 x 31	W16 x 26	W18 x 35	W18 x 35	W16 x 26	W16 x 31	W 16 x 31
3	W10 x 33	W21 x 44	W16 x 26	W14 x 22	W16 x 26	W14 x 22	W14 x 22	W16 x 26	W16 x 26	W 16 x 26
4	W8 x 18	W12 x 16	W12 x 16	W12 x 16	W12 x 14	W12 x 14	W12 x 16	W12 x 14	W14 x 22	W 12 x 16
5	W21 x 68	W14 x 30	W18 x 35	W21 x 48	W16 x 26	W16 x 26	W16 x 31	W21 x 44	W16 x 31	W 18 x 35
6	W24 x 55	W21 x 44	W18 x 35	W18 x 40	W18 x 40	W18 x 40	W21 x 44	W18 x 35	W18 x 40	W 18 x 35
7	W21 x 50	W14 x 22	W18 x 35	W16 x 31	W18 x 35	W18 x 35	W18 x 35	W18 x 35	W16 x 26	W 18 x 35
8	W12 x 40	W16 x 26	W16 x 26	W16 x 36	W14 x 22	W12 x 22	W16 x 26	W12 x 22	W14 x 22	W 16 x 26
w-*kN*	**41.02**	**33.9814**	**32.83**	**32.29**	**31.68**	**31.3786**	**31.243**	**31.05**	**30.91**	**30.788**

e) A five-story, two-bay frame

In this example a five-story frame with two bays is studied, Fig. 11. For all structural members, E and ρ are assumed to be 205.8 *GPa* and 78 kN/m^3, respectively. According to references [39,40], the allowable stress for all the structural members is equal to ±166.6 *MPa* and the allowable displacement for nodes of the last story is 1/500 of the frame height.

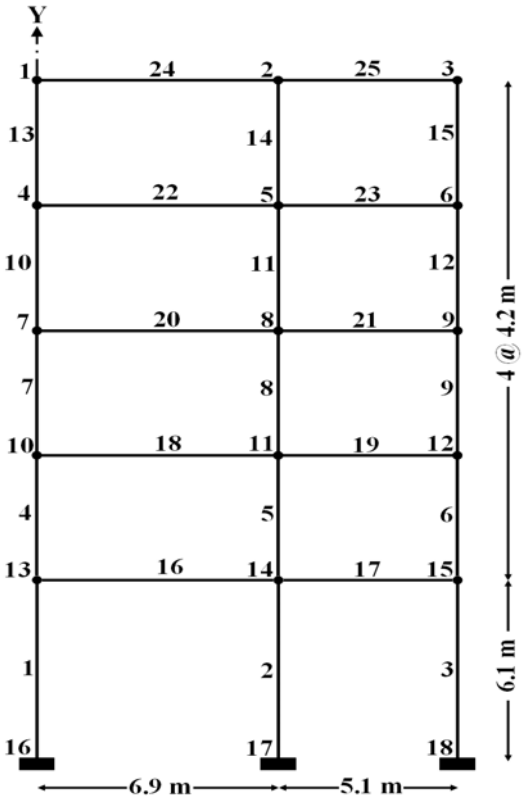

Fig. 11. A five-story, two-bay unbraced frame

Dead, live, and wind loads are applied to the structure as the following three cases (the magnitude and directions of the loads are defined in Table 8).

i) $DL+0.9(LL+WL)$ *ii*) $DL+WL$ *iii*) $DL+LL$

Table 8. Applied loads to the five-story, two-bay unbraced frame

Loading type	Magnitude and direction
Dead load	$W_y = -11.76$ *kN/m* on members 16 - 25
	$P_y = -19.6$ *kN* at nodes 1 and 3
	$P_y = -40.2$ *kN* at nodes 4, 6, 7, 9, 10, 12, 13 and 15
Live load	$W_y = -10.78$ *kN/m* on members 16 - 25
Wind load	P_x =5.684 *kN* at node 1
	P_x =7.252 *kN* at node 4
	P_x =6.664 *kN* at node 7
	P_x =5.978 *kN* at node 10
	P_x =6.272 *kN* at node 13

Columns must have a constant cross section in each story for the designed frame. On the other hand, since all the structural beams are designed independently, a total of 15 design variables are selected and considered from the list of sections of Table 9.

Table 9. Available cross-section for the five-story, two-bay unbraced frame

Section number	A cm^2	I_y cm^4	S_y cm^3	I_x cm^4	S_x cm^3	Section number	A cm^2	I_y cm^4	S_y cm^3	I_x cm^4	S_x cm^3
1	51.38	2545.50	282.83	1439	211.70	8	97.00	15021.30	938.83	4787	5444
2	57.66	3560.80	356.08	1872	256.40	9	109.80	16113.50	1007.10	5801	644.50
3	63.67	4787.70	435.25	2313	300.30	10	121.78	23748.20	1319.35	7147	744.50
4	69.81	6710.20	537.46	2647	339.40	11	136.18	25303.40	1405.75	8502	867.80
5	79.81	7239.10	579.13	3272	408.90	12	150.09	35155.40	1757.77	9646	964.60
6	80.04	9505.10	678.13	3420	417.10	13	166.09	37288.70	1864.44	11278	1105.70
7	91.24	10236.80	731.20	4192	499.10	14	182.09	39422.10	1971.10	12975	1247.62

In Fig. 12, the convergence curves for this example are illustrated for the proposed methods. Each curve is obtained using the average of 30 different runs. Therefore, the effect of random parameters on the proposed methods is reduced and more accurate judgment can be made. Results show that the HACOHS-T method has better performance than the other methods in obtaining the optimum design. Final design obtained from HACOHS-T method has lower weight compared to the other proposed methods and references.

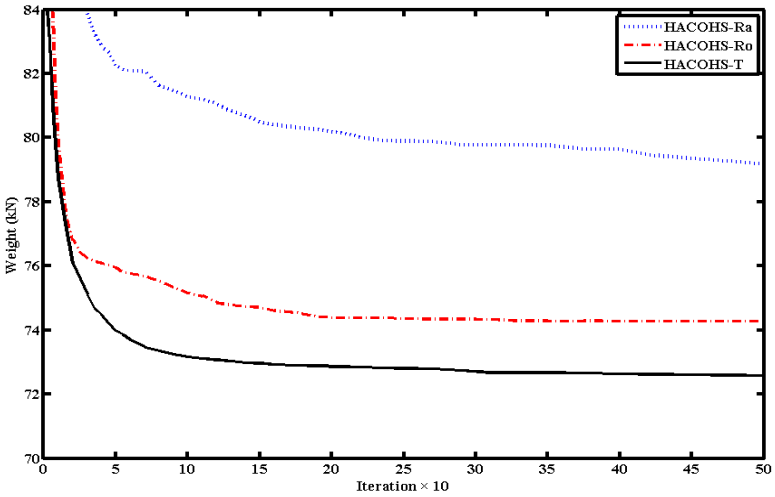

Fig. 12. The convergence history obtained with the proposed methods for the present frame after 30 runs

Table 10 includes the results of the optimum design of other references compared to those of the HACOHS-T method.

Table 10. Comparison of the optimal designs for the five-story, two-bay unbraced frame

Group	Member	Chai and Sun [39]	Juang and Chang [40]	This Study
		RDQA	DLM	HACOHS-T
1	1-3	80.04	80.04	80.04
2	4-6	80.04	69.81	69.81
3	7-9	69.81	69.81	69.81
4	10-12	69.81	63.67	69.81
5	13-15	69.81	63.67	51.38
6	16	80.04	97.00	80.04
7	17	80.04	69.81	97.00
8	18	80.04	80.04	80.04
9	19	69.81	69.81	69.81
10	20	80.04	80.04	80.04
11	21	69.81	69.81	57.66
12	22	69.81	80.04	80.04
13	23	69.81	57.66	57.66
14	24	69.81	80.04	80.04
15	25	69.81	63.67	69.81
	Weight-*kN*	**74.60**	**73.27**	**72.596**

4. CONCLUDING REMARKS

In this paper, a new combined method is proposed for optimal design of skeletal structures such as frames and trusses through combining the ACO, HS and GA selection methods. In this algorithm, the global and local search processes are simultaneously performed based on the above mentioned methods. The ACO method deals with global search process whereas HS method and ACO perform local search. On the other hand, different selection approaches consisting of Roulette Wheel (HACOHS-RO), Rank (HACOHS-RA) and Tournament (HACOHS-T) methods are used in the combined HACOHS algorithm. It is found that the HACOHS-T method has a better performance than the other methods. This can be easily observed from Figs. 4, 6, 8, 10 and 12.

It should be mentioned that the HACOHS-RO method also has appropriate convergence property in small search spaces with low number of cross list of sections, while in large search spaces this is not as successful as HACOHS-T method. Thus it is not advisable for problems with large search spaces.

On the other hand, having slow convergence rate, the HACOHS-Ra does not provide a proper process for the present problems to obtain optimum point. Therefore, applying this method is not recommended. Considering the quality of results, the proposed HACOHS-T method is superior to the other proposed methods and other existing algorithms. This point can also be observed form the results of the investigated examples consisting of the 8-story frame 1- bay, 5-story 2- bays and the 200-bar, 72-bar and 52-bar truss examples.

In all the optimized structures, the algorithms of some other researchers are also improved, and the HACOHS-T achieved a design of smaller weight. The advantages of GA, HS and ACO algorithms are used in HACOHS-T algorithm so that the search space is searched more accurately and the probability of being trapped in local optimum is reduced. Furthermore, the convergence of the HACOHS-T method indicates that the algorithm does not need the tuning of parameters of the constituting algorithms. According to HACOHS-T method, suitable cross sections are selected for the members based on the

tournament method of Genetic algorithm, and global and local search abilities of the ant colony algorithm and Harmony search are simultaneously utilized.

***Acknowledgement*:** The second author is grateful to the Iran National Science Foundation for support.

REFERENCES

1. Glover, F. & Kochenberger, G. A. (2003). Handbook of metaheuristics. Kluwer Academic Publishers, Boston, USA.
2. Dreo, J., Petrowski, A., Siarry, P. & Taillard, E. (2006). *Metaheuristics for hard optimization*. Springer-Verlag, Berlin, Heidelberg, Germany.
3. Fogel, L. J, Qwens, A. J. & Walsh, M. J. (1966). *Artificial intelligence through simulated evolution*. John Wiley & Sons, Chichester, UK.
4. Holland, J. H. (1975). *Adaptation in natural and artificial system*. University of Michigan Press, Ann Arbor, MI, USA.
5. Goldberg, D. E. (1989). *Genetic algorithm in search optimization and machine learning*. Addision-Wesley, Boston, USA.
6. Colorni, A., Dorigo, M. & Maniezzo, V. (1991). Distributed optimization by ant colony. *In: Proceeding of the first European conference on artificial life*, USA, pp. 134-142.
7. Dorigo, M. (1992). Optimization learning and natural algorithm (in Italian). PhD. Thesis, Diparimento di, Elettronica, Politecnico di Milano, Milan, Italy.
8. Geem, Z. W., Kim, J. H. & Loganathan, G. V. (2001). A new heuristic optimization algorithm: harmony search. *Int J Model Simulat*, Vol. 76, No. 2, pp. 60-68.
9. Kaveh, A. & Talatahari, S. (2007). A discrete particle swarm ant colony optimization for design of steel frames. *Asian J Civil Eng*, Vol. 9, No. 6, pp. 563-575.
10. Kao, Y. T. & Zahra, E. (2008). A hybrid genetic algorithm and particle swarm optimization for multimodal function. *Appl Soft Comput*, Vol. 8, No. 2, pp. 849-857.
11. Kaveh, A. & Talatahri, S. (2009). A particle swarm ant colony optimization for truss structures with discrete variables. *J Construct Steel Res*, Vol. 65, Nos. (8-9), pp. 1558-1568.
12. Kaveh, A. & Malakoutirad, S. (2010). Hybrid genetic algorithm and particle swarm optimization for the force method-based simultaneous analysis and design. *Iranian J Sci Tech*, Vol. 34, pp. 15-34.
13. Camp, C. V. & Bichon, J. B. (2004). Design of space trusses using ant colony optimization. *J Struct Eng ASCE*, Vol. 130, No. 5, pp. 741-751.
14. Camp, C. V., Bichon, J. B. & Stovall, S. P. (2004). Design of steel frames using ant colony optimization, *J Struct Eng ASCE*, Vol. 131, No. 3, pp. 369-379.
15. Kaveh, A. & Shojaee, S. (2007). Optimal design of skeletal structures using ant colony optimization. *Int J Numer Methods Eng*, Vol. 70, No. 5, pp. 563-581.
16. Capriles, V. S. Z., Fonseca, L. G., Barbosa, H. J. C. & Lemonge, A.C.C. (2007). Rank-based ant colony algorithms for truss weight minimization with discrete variables. *Commun Numer Methods Eng*, Vol. 23, No. 6, pp. 553-575.
17. Kaveh, A. & Talatahari, S. (2010). An improved ant colony optimization for the design of planar steel design frames. *Eng Struct*, Vol. 32, No. 3, pp. 864-873.
18. Kaveh A. & Talatahari S. (2010). An improved ant colony optimization for constrained engineering design problems. *Eng Comput*, Vol. 27, No. 1, pp. 155-182.
19. Stützle, T. & Hoos, H. (1997). Improvement on the ant system: Introducing MAX-MIN ant system. *Proceeding of the international conference on artificial neural network and genetic algorithm*, Wien, pp. 245-249.

20. Bullnheimer, B., Hart, R. F. & Strauss, C. (1997). A new rank-based version of the ant system: a computational study. Technical Report POM-03/97, Institute of Management Science, University of Vienna, Austria.
21. Cordón, O., Herrera, F. & Stützle, T. (2002). A review on ant colony optimization metaheuristic: basic, models and new trends. *Math Soft Comput*, Vol. 9, Nos. 2-3, pp. 141-175.
22. Lee, K. S. & Geem, Z. W. (2005). A new meta-heuristic algorithm for continuous engineering optimization. Harmony search theory and practice, *Comput Methods Appl Mech Eng*, Vol. 194, Nos. 36-38, pp. 3902-3933.
23. Lee, K. S. & Geem, Z. W. (2004). A new structural optimization method based on the harmony search algorithm. *Comput Struct*, Vol. 82, Nos. 9-10, pp. 781-798.
24. Kalatjari, V. R. & Talebpour, M. H. (2011). Optimization of structures cross-section and topology by genetic algorithm and examination of different methods affect of selection process on optimization procedure. *Proceedings of the 6th National Congress on Civil Engineering*, Semnan University, Semnan, Iran, p. 26.
25. Hasançebi O., Çarbaş, S., Doğan, E., Erdal, F. & Saka, M. P. (2009). Performance evaluation of metaheuristic search techniques in the optimum design of real size pin jointed structures. *Comput Struct*, Vol. 87, Nos. 5-6, pp. 284-302.
26. Haupt, R. L. & Haupt, E. (2001). *Practical genetic algorithms*. John Wiley & Sons, 2nd ed. New York, USA.
27. Mitchell, M. (1998). *An introduction to genetic algorithms*. MIT Press, Cambridge, USA.
28. Yang, J. & Soh, C. K. (1997). Structural optimization by genetic algorithms with tournament selection. *J Comput Civil Eng ASCE*, Vol. 11, No. 3, pp. 195-200.
29. Kalatjari, V. R. & Talebpour, M. H. (2011). Sizing and topology optimization of truss structures by modified multi-search-method. *J Civil Surveying Eng*, Vol. 45, No. 3, pp. 351-363.
30. Lee, K. S., Geem, Z. W., Lee, S. H. & Bae, K. W. (2005). The harmony search heuristic algorithm for discrete structural optimization. *Eng Optim*, Vol. 37, No. 7, pp. 663-684.
31. Wu, S. J. & Chow, P. T. (1995). Steady-state genetic algorithm for discrete optimization of trusses. *Comput Struct*, Vol. 56, No. 6, pp. 979-991.
32. Li, L. J., Huang, Z. B. & Liu, F. (2009). A heuristic particle swarm optimization method for truss structures with discrete variables. *Comput Struct*, Vol. 87, Nos. 7-8, pp. 435-443.
33. Kaveh, A. & Talatahri, S. (2010). A charged system search with a fly to boundary method for discrete optimum design of truss structures. *Asian J Civil Eng*, Vol. 11, No. 3, pp. 277-293.
34. Coello, C. A. & Christiansen, A. D. (2000). Multiobjective optimization of trusses using genetic algorithms. *Comput Struct*, Vol. 75, No. 6, pp. 647-660.
35. Toğan, V. & Daloğlu, T. A. (2008). An improved genetic algorithm with initial population strategy and self-adaptive member grouping. *Comput Struct*, Vol. 86, Nos. 11-12, pp. 1204-1218.
36. Kalatjari, V. R. & Talebpour, M. H. (2009). Reducing the effect of GA parameters on optimization of topology and cross section for truss structures using multi-search-method. *J Techn Edu*, Vol. 4, No. 1, pp. 57-72.
37. Khot, N. S., Venkayya, V. B. & Berke, L. (1976). Optimum structural design with stability constraints. *Int J Numer Methods Eng*, Vol. 10, No. 5, pp. 1097-1114.
38. Camp, C. V., Pezeshk, S. & Cao, G. (1998). Optimized design of two dimensional structures using a genetic algorithm. *J Struct Eng ASCE*, Vol. 124, No. 5, pp. 551-559.
39. Chai, S. & Sun, H. G. (1996). A relative difference quotient algorithm for discrete optimization, *Struct Optim*, Vol. 12, No. 1, pp. 46-56.
40. Juang, D. S. & Chang, W. T. (2006). A revised discrete lagrangian-based search algorithm for the optimal design of skeletal structures using available section. *Struct Multidiscip Optim*, Vol. 31, No. 3, pp. 201-210.